Optimizing Subsurface Characterization: A Flow Zone Indicator Framework for Improved Permeability Modeling

Mohamed Abdelwahab Ataallah
Department of Hydrogeology and Environment
Faculty of Earth Sciences, Beni-Suef University
Beni-Suef, Egypt
dr.m.a.ataallah@gmail.com

***Abstract*— This study introduces a robust and comprehensive framework for characterizing and predicting permeability in heterogeneous reservoirs by leveraging the Flow Zone Indicator (FZI) concept. We demonstrate that while a single global porosity-permeability relationship provides a limited understanding (R2 equal 0.6493), it fails to capture the intricate, multi-scale heterogeneity that governs fluid flow. Our methodology successfully delineates the reservoir into five distinct hydraulic flow units (FZI 0 to 4), each exhibiting a unique and highly predictive exponential relationship between porosity and permeability. The remarkably high coefficients of determination within these units (e.g., R2 equal 0.9479 for FZI 0) provide compelling evidence that FZI effectively segregates the reservoir into truly homogeneous domains. This approach enables the development of unit-specific predictive models that are significantly more accurate than a single bulk-rock correlation. Furthermore, the validation of core porosity against log porosity allows for the generation of high-resolution, continuous permeability profiles across uncored intervals, which is crucial for comprehensive reservoir characterization. This work affirms that the FZI method is an indispensable tool for advanced reservoir petrophysics, moving beyond simplistic correlations to unlock a granular understanding of reservoir quality. The resulting precise permeability models are fundamental for optimizing well placement, improving fluid flow simulations, and designing more effective enhanced oil recovery (EOR) strategies. This methodology has broader implications for sustainable development, aligning with Sustainable Development Goals (SDG) 9: Industry, Innovation, and Infrastructure by enhancing resource efficiency and supporting cleaner energy applications like carbon capture and storage (CCUS) and geothermal energy.**

Keywords — FZI framework fundamentally enhances permeability prediction in heterogeneous reservoirs; Five distinct hydraulic flow units (FZI 0-4) with unique, highly predictive exponential porosity-permeability relationships are delineated; Unit-specific FZI models significantly outperform conventional bulk-property correlations for permeability estimation; Validated log porosity enables high-resolution permeability profiles in uncored intervals; FZI is an indispensable tool for optimizing reservoir management and enhancing hydrocarbon recovery

I. INTRODUCTION

Permeability is a crucial parameter in reservoir characterization and predicting its 3D distribution in heterogeneous reservoirs is a challenging task. A poor prediction of permeability will result in inefficient and unreliable dynamic models, thus, reducing the accuracy of these models for describing and modelling the past, current and future performance of oil and gas reservoirs.

The classical approach in the oil industry was to predict permeability from a single well log attribute. The Kozeny Carman or Wyllie and Rose equations [1] were often used to predict permeability from a porosity log. These equations have adjustable variables with values depending on the sorting and geometry of rock grains. [2] reported that by including other well log attributes than porosity and using multiple linear regression approach, the correlation coefficient between the estimated and actual permeability increases. [3] have made similar suggestions. They suggested that instead of using a single well log, a group of several logs provide a better permeability prediction because of the existing correlations between permeability and other well log parameters. Lacentre and [4]; [5] introduced a method to estimate permeability based on well logs and core data. Many other researchers also attempted to establish mathematical relations between permeability and other petrophysical parameters and well logs by using statistical methods such as multivariate regression analysis and proxy modeling [6].

The findings from this research were significant in identifying influential parameters on permeability but were not successful to provide a general workflow for accurate prediction of permeability in all reservoirs and their applicability should also be checked in other field studies. Although these techniques have provided good results in some cases, they require the existence of many core measurements, which is expensive to achieve in practice. In addition, the accuracy of these correlations diminishes when dealing with heterogeneous reservoirs.

Recently, intelligent approaches including artificial neural networks (ANNs), fuzzy clustering and least square support vector machines (LSSVM) have been proven as effective tools for prediction of reservoir permeability. [7] developed a rule based fuzzy model for the prediction of petrophysical rock parameters. [8] used neural network and fuzzy logic modeling for estimation of porosity and permeability in a reservoir, revealing that these methods have potential for future use and implementation. [9] have successfully applied machine learning methods for permeability prediction and achieved acceptable results. [10] compared ANN with seven conventional empirical equations for prediction of permeability in a tight carbonate

ISSN: 2636 - 3712 (Printed Version)
ISSN: 2636 - 3720 (Online Version)

reservoir. They also used the genetic algorithm to develop a new empirical equation for prediction of permeability based on their dataset. Their results showed that the machine learning methods provide better predictions in comparison with empirical equations. [11] predicted permeability from well logs using a new hybrid machine learning algorithm. Their research combined Social Ski-Driver (SSD) algorithm with the multilayer perception (MLP) neural network and presented a new hybrid algorithm to predict rock permeability. Their results indicated that the hybrid models can deliver satisfactory results.

Models developed based on hydraulic flow units (HFU) provide a better permeability prediction compared to other ones. Flow Zone Indicator (FZI) which is calculated according to rock porosity and permeability is strongly related to HFU. Rock samples, which belong to the same HFU, have similar FZI ranges. While HFU is a parameter used for classification, FZI is a quantitative parameter, which makes it suitable for developing prediction models. In the past, different researchers [12], [13] developed models to predict FZI, and then applied the predicted FZI to calculate permeability. [14] implemented a fuzzy model for estimation of permeability by grouping the data into different HFUs using the FZI values and managed to predict permeability accurately.

A neural network model was proposed by [15] to identify various flow units and estimate the permeability of a reservoir. [16] developed an ANN model for prediction of permeability in different rock types of a heterogeneous carbonate reservoir. [17] utilized the support vector machine (SVM) and proposed an approach to predict the FZI values in a carbonate reservoir by using well log data as parameters. Although there are different research works in the literature on application of regression and machine learning approaches for prediction of permeability, few papers are available on prediction of permeability in tight carbonate gas condensate reservoirs, which are among the most challenging reservoirs to develop in the world [18], [19].

Since developing new methodologies to accurately predict permeability is important, further analysis and examination of machine learning and regression methods to find reliable, fast and accurate models are of great importance.

In this study, we are presenting a novel approach based on artificial neural networks (ANN) to predict the 3D distribution of permeability in heterogeneous tight gas condensate reservoirs using petrophysical log data and FZI from core data. The S field is a natural gas field, which consists of five main gas bearing S reservoirs, namely S1, S2, S3, S4 and S5 with similar rock properties. These five reservoirs are isolated by impermeable barriers but based on the observed pressure analysis, they are communicating through faults.

II. Methodology

A. Statistical distribution for petrophysical parameters using the Geographic Information System (GIS) and Histogram with normal distribution.

B. . Scatter plotting for core porosity and core permeability

C. Making the relationship between core porosity and log porosity

D. Flow Zone Indicator Method (FZI) and Rock Quality Index (RQI).

Rock typing is a process in which S reservoir rocks are classified into distinct units. One of the frequently used approaches for rock typing is the FZI method. [20] introduced this method for the first time. This technique identifies existing trends between permeability and porosity using the FZI values of S reservoir rocks. The general Kozeny-Carman relation for calculating permeability is given by Equation (1), which is (1)K=1014Øe3(1−Øe)2[1Fsτ2Sgv2] where, K is core permeability in mD, Øe is effective core porosity, Fs denotes shape factor, τ is tortuosity and Sgv represents the surface area per grain volume. Calculation of permeability by this equation is not an easy task because it is difficult to measure the Fs, τ and Sgv parameters for reservoir rocks. [20] defined the FZI as the square root of the 1/Fsτ2Sgv2 term and derived Eq. (2) to obtain FZI from core data:(2)FZI=RQIØn(3)ØRQI=0.0314KØe(4)ØØØØn=Øe1−Øe where, RQI is a parameter called reservoir quality index (μm) and Øn is the normalized porosity. The calculated FZI is then used to group the rocks into discrete rock types (DRTs) according to the following relation:(5)DRT=Round(2Log(FZI)+10.6).

E. Predicted permeability using correlation coefficient R2 between core porosity and core permeability and applying it between log porosity and log permeability

F. Using Microsoft Excel software.

III. Results

A. Statistical of Core Permeability and Core Porosity

The core data of S well was used in this study for rock typing based on the FZI approach. The statistical parameters of the core porosity and permeability statistical is summarized in Table 1.

From the histogram for porosity shown in Figure 1a, a unimodal porosity distribution is observed with a minimum and maximum porosity values of 0.076 and 0.354 (m3/m3) respectively. Figure 1c shows a histogram of the permeability across the field with the data range of 0.16–2054 (mD). The wide range of permeability distribution on this histogram indicates that the understudy gas field is very heterogeneous and for an accurate permeability prediction, clustering the core data into appropriate Discreet Rock Texture (DRT) groups is essential.

1) Core Property Distributions (Porosity)

The statistical distributions of core porosity and permeability were analysed using histograms, as presented in Figure 1.

TABLE I. THE STATISTICAL PARAMETERS OF THE CORE POROSITY (FRACTION) AND PERMEABILITY (MD). IT ILLUSTRATES CORE PLUGS, MINIMUM (MIN), MAXIMUM (MAX), AVERAGE, AND STANDARD DEVIATION (STD. DEVIATION) FOR EACH OF POROSITY AND PERMEABILITY.

Parameter	Core plugs	Min	Max	Average	Std. Deviation
Porosity	101	0.076	0.354	0.213	0.0774
Permeability	101	0.16	2054	199	404

Figure 1a (Core Porosity Histogram using GIS) and Figure 1b (Core Porosity Histogram with normal distribution) illustrate the frequency distribution of core porosity values. The histogram reveals a range of porosity values, with a peak indicating the most frequent porosity range within the S reservoir. While Figure 1b attempts to fit a normal distribution curve, deviations from perfect normality suggest inherent variability in the pore volume across the samples.

2) Core Property Distributions (Permeability)

Figure 1c (Core Permeability Histogram using GIS) and Figure 1d (Core Permeability Histogram with normal distribution) display the frequency distribution of core permeability values. Permeability typically spans several orders of magnitude in S reservoir rocks, and its histogram often exhibits a log-normal distribution rather than a simple normal distribution. The spread observed in these histograms highlights the significant heterogeneity of permeability within the S reservoir, which is a primary challenge for accurate flow modelling.

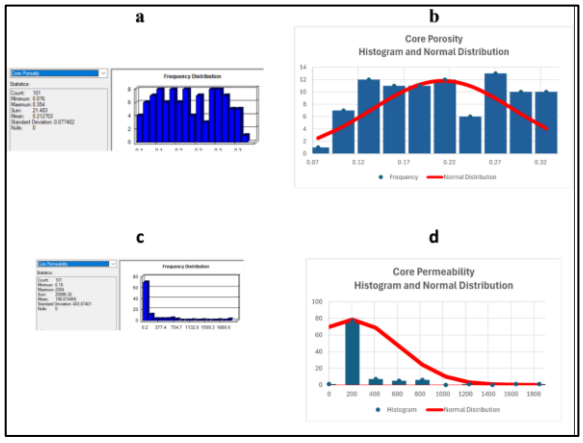

Fig. 1. *a. Core Porosity Histogram using GIS, b. Core Porosity Histogram with normal distribution, c. Core permeability Histogram using GIS, d. Core permeability Histogram with normal distribution.*

3) Core Porosity versus Core Permeability

Figure 2 presents the scatter plot illustrating the overall relationship between core porosity (x-axis, linear scale) and core permeability (y-axis, logarithmic scale) for all available core samples from the S reservoir. A general positive exponential trend is clearly observed, indicating that as core porosity increases, core permeability also tends to increase, but at an accelerating rate. An exponential regression model was fitted to this entire dataset, yielding the following equation: y = 0.0436e29.438x . Where; y represents the core permeability (in mD), x represents the core porosity (in a fraction), and e is Euler's number. The coefficient of determination (R2) for this fitted model is 0.6493. This indicates that approximately 64.93% of the variability in core permeability can be explained by core porosity when considering the entire reservoir as a single petrophysical unit.

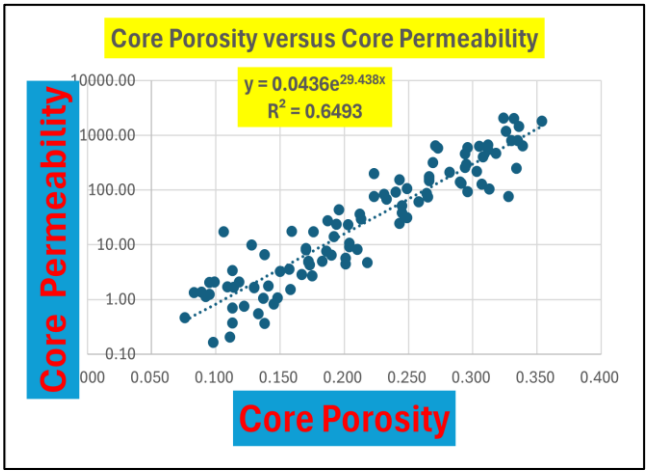

Fig. 2. *Core Porosity Versus Core Permeability. It illustrates scatter plot illustrating the overall relationship between core porosity (x-axis, linear scale) and core permeability (y-axis, logarithmic scale) for all available core samples from the S reservoir..*

B. . Prediction of Permeability in Uncored intervals

1) Core and Log data

Table 2 presents the input data utilized in this study, comprising core porosity, core permeability, and log porosity measurements. The dataset includes paired measurements of core porosity (in percent and decimal fraction), core permeability (in mD), and corresponding log porosity (in percent and decimal fraction) for numerous samples. The core porosity values range approximately from 7.6% to 35.4%, while core permeability spans a wide range, from as low as 0.16 mD to as high as 2054 mD, indicating significant variability in S reservoir quality. A visual inspection of the data suggests a general positive relationship between core porosity and core permeability, where higher porosity values tend to correspond with higher permeability values. A direct comparison between core porosity and log porosity reveals a strong agreement between the two measurements. For instance, a core porosity of 11.1% (0.111 decimal) is consistently matched by a log porosity of 11.10% (0.11 decimal). This high degree of congruence is observed across the entire dataset, suggesting that the log porosity measurements accurately reflect the core-derived porosity values.

2) Core and Log data

Table 3 presents the calculated petrophysical parameters, including Rock Quality Index (RQI), Average Porosity (PHIZ), Flow Zone Indicator (FZI), and the resulting Predicted Permeability, along with their respective FZI ranges. These parameters were derived from the input core and log data. The Rock Quality Index (RQI) values vary from approximately 0.04 to 2.50, reflecting a wide spectrum of rock qualities within the S reservoir. The Average Porosity (PHIZ) values, representing the

effective porosity, range from about 0.08 to 0.55. The calculated Flow Zone Indicator (FZI) values span a broad range, from approximately 0.32 to 5.22. These FZI values were systematically categorized into distinct FZI ranges: 0-0.5, 0.5-1, 1-1.5, 1.5-2, 2-2.5, 2.5-3, 3-3.5, 3.5-4, 4-4.5, and 4.5-5. This categorization demonstrates the successful delineation of multiple hydraulic flow units (HFUs) within the reservoir. Corresponding to these FZI values and ranges, the Predicted Permeability values exhibit a wide distribution, ranging from as low as 0.41 mD to as high as 1820 mD. A clear trend is observed where higher FZI values generally correspond to significantly higher predicted permeabilities, indicating a strong correlation between the FZI and the rock's fluid flow capacity.

3) C Flow Zone Indicator (FZI) FZI 0, 1, 2, 3, and 4

Flow Zone Indicator (FZI) Based Porosity-Permeability Relationships in figure 3 which presents a composite scatter plot illustrating the relationship between core porosity (x-axis, linear scale) and core permeability (y-axis, logarithmic scale) for all identified Flow Zone Indicator (FZI) groups: FZI 0, FZI 1, FZI 2, FZI 3, and FZI 4. Each FZI group is distinctly color-coded, and its unique exponential regression trendline, equation, and coefficient of determination (R^2) are displayed.

The analysis of each FZI group yielded the following specific 5 exponential relationships:

1. FZI 0: y=0.0412e24.921x (R^2 =0.9479)
2. FZI 1: y=0.2994e 21.182x (R^2 =0.8217)
3. FZI 2: y=1.4823e 18.253x (R^2 =0.8444)
4. FZI 3: y=3.4714e 17.21x (R^2 =0.7898)
5. FZI 4: y=19.534e 13.387x (R^2 =0.5234)

Visually, figure 3 clearly demonstrates that the data points for each FZI group cluster distinctly, forming separate, parallel-like trends on the semi-log plot. There is a clear upward progression of these trendlines from FZI 0 to FZI 4, indicating increasing permeability for a given porosity as the FZI number increases. The R^2 values for FZI 0, FZI 1, FZI 2, and FZI 3 are consistently high (above 0.78), signifying strong correlations within these groups. FZI 4, while showing a positive trend, exhibits a lower R^2 value.

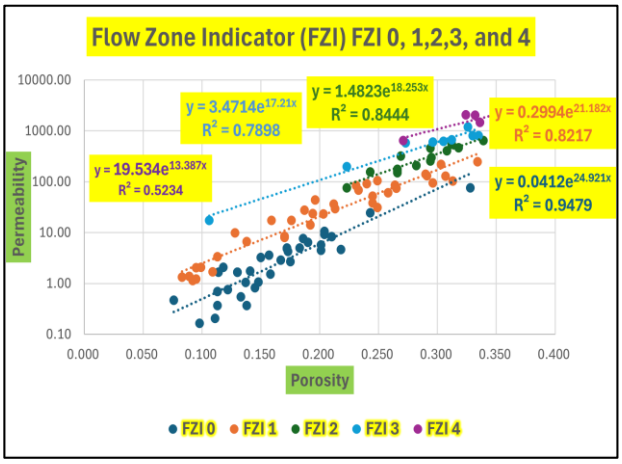

Fig. 3. *Flow Zone Indicator (FZI) FZI 0, FZI 1, FZI 2, FZI 3, and FZI 4. It clearly demonstrates that the data points for each FZI group cluster distinctly, forming separate, parallel-like trends on the semi-log plot..*

4) Predicted Permeability versus Core Permeability

Figure 4 presents a cross-plot comparing the Predicted Permeability (x-axis, logarithmic scale) against the actual Core Permeability (y-axis, logarithmic scale). The data points generally align along a diagonal trend, indicating a positive correlation between the predicted and measured values. A linear regression analysis was performed on the logarithmically scaled data, yielding the following relationship: y=1.001x 1 . This equation, effectively y=x, represents the ideal one-to-one correlation where predicted values perfectly match actual values. The coefficient of determination (R^2) for this relationship is 0.6493. This value indicates that approximately 64.93% of the variability in core permeability can be explained by the predicted permeability.

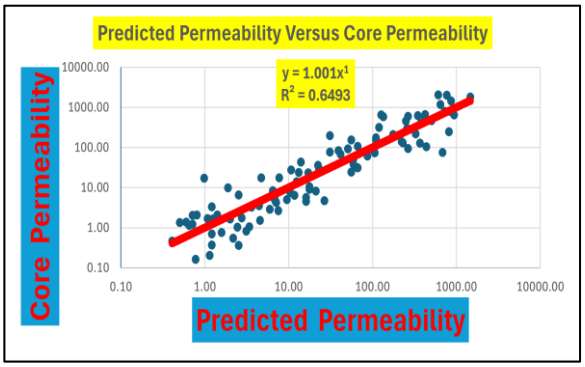

Fig. 4. *Predicted Permeability Versus Core Permeability. It presents a cross-plot comparing the Predicted Permeability (x-axis, logarithmic scale) against the actual Core Permeability (y-axis, logarithmic scale)..*

TABLE II. INPUT DATA CONTAINS CORE POROSITY, CORE PERMEABILITY, AND LOG POROSITY.

Core Porosity Percent	Core Permeability	Core Porosity Decimal	Log Porosity Percent	Log Porosity Decimal
11.1	0.21	0.111	11.10	0.11
13.8	0.37	0.138	13.80	0.14

Core Porosity Percent	Core Permeability	Core Porosity Decimal	Log Porosity Percent	Log Porosity Decimal
9.8	0.16	0.098	9.80	0.10
13.3	0.55	0.133	13.30	0.13
14.5	0.83	0.145	14.50	0.14
11.3	0.37	0.113	11.30	0.11
14.8	1.06	0.148	14.80	0.15
15.8	1.52	0.158	15.80	0.16
21.8	4.68	0.218	21.80	0.22
13.7	1.04	0.137	13.70	0.14
12.2	0.76	0.122	12.20	0.12
17.5	2.68	0.175	17.50	0.17
20.1	4.49	0.201	20.10	0.20
11.3	0.70	0.113	11.30	0.11
16.7	2.86	0.167	16.70	0.17
20.1	5.71	0.201	20.10	0.20
14.1	1.76	0.141	14.10	0.14
18.3	4.99	0.183	18.30	0.18
21.0	8.28	0.210	21.00	0.21
17.3	4.28	0.173	17.30	0.17
13.0	1.65	0.130	13.00	0.13
13.0	1.67	0.130	13.00	0.13
19.0	6.47	0.190	19.00	0.19
17.2	4.81	0.172	17.20	0.17
15.7	3.58	0.157	15.70	0.16
17.2	4.99	0.172	17.20	0.17
20.4	9.17	0.204	20.40	0.20
15.0	3.24	0.150	15.00	0.15
18.6	7.60	0.186	18.60	0.19
20.4	10.6	0.204	20.40	0.20
11.4	1.66	0.114	11.40	0.11
7.6	0.47	0.076	7.60	0.08
32.8	75.9	0.328	32.80	0.33
24.3	24.4	0.243	24.30	0.24
11.8	2.07	0.118	11.80	0.12
10.9	1.70	0.109	10.90	0.11
17.0	8.06	0.170	17.00	0.17
24.9	31.1	0.249	24.90	0.25
9.5	1.23	0.095	9.50	0.09

Core Porosity Percent	Core Permeability	Core Porosity Decimal	Log Porosity Percent	Log Porosity Decimal
17.0	8.47	0.170	17.00	0.17
9.2	1.14	0.092	9.20	0.09
19.2	14.1	0.192	19.20	0.19
24.5	38.4	0.245	24.50	0.24
31.3	104	0.313	31.30	0.31
8.9	1.37	0.089	8.90	0.09
9.9	2.07	0.099	9.90	0.10
20.3	23.4	0.203	20.30	0.20
29.6	94.2	0.296	29.60	0.30
11.3	3.36	0.113	11.30	0.11
13.8	6.62	0.138	13.80	0.14
21.3	29.7	0.213	21.30	0.21
9.5	2.05	0.095	9.50	0.09
25.8	61.2	0.258	25.80	0.26
8.3	1.34	0.083	8.30	0.08
24.5	52.1	0.245	24.50	0.24
19.4	23.7	0.194	19.40	0.19
30.7	129	0.307	30.70	0.31
26.5	74.3	0.265	26.50	0.26
17.6	17.4	0.176	17.60	0.18
21.2	36.1	0.212	21.20	0.21
26.4	86.1	0.264	26.40	0.26
29.1	132	0.291	29.10	0.29
18.7	27.5	0.187	18.70	0.19
29.0	141	0.290	29.00	0.29
33.4	249	0.334	33.40	0.33
15.9	17.5	0.159	15.90	0.16
23.3	68.6	0.233	23.30	0.23
12.8	9.83	0.128	12.80	0.13
19.6	43.7	0.196	19.60	0.20
30.3	218	0.303	30.30	0.30
24.0	91.9	0.240	24.00	0.24
24.9	106	0.249	24.90	0.25
23.1	83.7	0.231	23.10	0.23
22.3	76.4	0.223	22.30	0.22
26.6	150	0.266	26.60	0.27
26.6	163	0.266	26.60	0.27

Core Porosity Percent	Core Permeability	Core Porosity Decimal	Log Porosity Percent	Log Porosity Decimal
28.2	210	0.282	28.20	0.28
26.6	175	0.266	26.60	0.27
29.4	257	0.294	29.40	0.29
29.5	297	0.295	29.50	0.29
24.3	155	0.243	24.30	0.24
30.8	406	0.308	30.80	0.31
31.8	468	0.318	31.80	0.32
33.9	648	0.339	33.90	0.34
31.2	546	0.312	31.20	0.31
26.9	318	0.269	26.90	0.27
29.4	462	0.294	29.40	0.29
33.5	808	0.335	33.50	0.33
33.0	807	0.330	33.00	0.33
31.2	665	0.312	31.20	0.31
30.5	629	0.305	30.50	0.30
22.3	199	0.223	22.30	0.22
29.6	600	0.296	29.60	0.30
10.6	17.4	0.106	10.60	0.11
27.3	585	0.273	27.30	0.27
32.6	1189	0.326	32.60	0.33
33.6	1458	0.336	33.60	0.34
35.4	1820	0.354	35.40	0.35
27.1	647	0.271	27.10	0.27
33.2	2030	0.332	33.20	0.33
32.4	2054	0.324	32.40	0.32

TABLE III. OUTPUT DATA CONTAINING ROCK QUALITY INDEX (RQI), AVERAGE POROSITY (PHIZ), FLOW ZONE INDICATOR (FZI), AND PREDICTED PERMEABILITY. COLORS INDICATES FZI DIFFERENT ZONES.

Rock Quality Index (RQI)	Porosity PHIZ	Flow Zone Indicator (FZI)	FZI Range	Predicted Permeability
0.042672	**0.124859**	**0.341762**	**0-0.5**	**1.14**
0.051136	**0.160093**	**0.319418**	**0-0.5**	**2.53**
0.04062	**0.108647**	**0.373869**	**0-0.5**	**0.78**
0.063795	**0.153403**	**0.41587**	**0-0.5**	**2.19**
0.07508	**0.169591**	**0.442712**	**0-0.5**	**3.11**
0.056972	**0.127396**	**0.447205**	**0-0.5**	**1.21**
0.084223	**0.173709**	**0.484854**	**0-0.5**	**3.40**

Rock Quality Index (RQI)	Porosity PHIZ	Flow Zone Indicator (FZI)	FZI Range	Predicted Permeability
0.097424	0.187648	0.519183	0.5 - 1	4.57
0.145456	0.278772	0.521773	0.5 - 1	26.70
0.08668	0.158749	0.546022	0.5 - 1	2.46
0.07832	0.138952	0.563645	0.5 - 1	1.58
0.122879	0.212121	0.579287	0.5 - 1	7.53
0.148407	0.251564	0.589937	0.5 - 1	16.19
0.078152	0.127396	0.613458	0.5 - 1	1.21
0.129943	0.20048	0.648161	0.5 - 1	5.95
0.167315	0.251564	0.665099	0.5 - 1	16.19
0.110937	0.164144	0.67585	0.5 - 1	2.77
0.163966	0.22399	0.732024	0.5 - 1	9.53
0.197167	0.265823	0.741725	0.5 - 1	21.10
0.156163	0.20919	0.746513	0.5 - 1	7.10
0.111968	0.149425	0.749325	0.5 - 1	2.00
0.112542	0.149425	0.753168	0.5 - 1	2.00
0.183234	0.234568	0.781154	0.5 - 1	11.71
0.166119	0.207729	0.799688	0.5 - 1	6.89
0.149941	0.18624	0.805099	0.5 - 1	4.43
0.169128	0.207729	0.814175	0.5 - 1	6.89
0.210523	0.256281	0.821452	0.5 - 1	17.68
0.145934	0.176471	0.826959	0.5 - 1	3.61
0.200689	0.228501	0.878283	0.5 - 1	10.41
0.226343	0.256281	0.883182	0.5 - 1	17.68
0.119672	0.128668	0.930086	0.5 - 1	1.25
0.077669	0.082251	0.944295	0.5 - 1	0.41
0.477654	0.488095	0.978609	0.5 - 1	680.57
0.314645	0.321004	0.980192	0.5 - 1	55.74
0.131451	0.133787	0.982541	0.5 - 1	1.41
0.124005	0.122334	1.013659	1-1.5	1.08
0.216208	0.204819	1.055606	1-1.5	6.50
0.350752	0.331558	1.057892	1-1.5	66.51
0.112985	0.104972	1.07633	1-1.5	0.71
0.221639	0.204819	1.082122	1-1.5	6.50
0.110532	0.101322	1.090903	1-1.5	0.65
0.269371	0.237624	1.133601	1-1.5	12.42
0.393108	0.324503	1.211415	1-1.5	59.12
0.572366	0.455604	1.25628	1-1.5	437.63

Rock Quality Index (RQI)	Porosity PHIZ	Flow Zone Indicator (FZI)	FZI Range	Predicted Permeability
0.123196	0.097695	1.261024	1-1.5	0.60
0.14372	0.109878	1.307995	1-1.5	0.80
0.337124	0.254705	1.323585	1-1.5	17.17
0.560156	0.420455	1.332264	1-1.5	265.31
0.171222	0.127396	1.344018	1-1.5	1.21
0.21748	0.160093	1.358461	1-1.5	2.53
0.370782	0.270648	1.369977	1-1.5	23.05
0.145863	0.104972	1.389536	1-1.5	0.71
0.48361	0.347709	1.390848	1-1.5	86.68
0.126166	0.090513	1.393908	1-1.5	0.50
0.457895	0.324503	1.411063	1-1.5	59.12
0.347059	0.240695	1.441904	1-1.5	13.17
0.643658	0.443001	1.452948	1-1.5	366.77
0.525776	0.360544	1.458286	1-1.5	106.52
0.312211	0.213592	1.461714	1-1.5	7.76
0.409747	0.269036	1.52302	1.5-2	22.38
0.56706	0.358696	1.580895	1.5-2	103.43
0.66876	0.410437	1.629384	1.5-2	229.00
0.380781	0.230012	1.655481	1.5-2	10.72
0.692373	0.408451	1.69512	1.5-2	222.36
0.857346	0.501502	1.709558	1.5-2	812.05
0.329326	0.189061	1.741907	1.5-2	4.70
0.538783	0.303781	1.77359	1.5-2	41.53
0.27517	0.146789	1.874597	1.5-2	1.89
0.468805	0.243781	1.923059	1.5-2	13.97
0.842241	0.43472	1.937433	1.5-2	326.03
0.614443	0.315789	1.945737	1.5-2	51.03
0.647863	0.331558	1.953995	1.5-2	66.51
0.597704	0.30039	1.98976	1.5-2	39.15
0.581198	0.287001	2.02507	2-2.5	30.94
0.7454	0.362398	2.056857	2-2.5	109.70
0.777289	0.362398	2.144851	2-2.5	109.70
0.85687	0.392758	2.181675	2-2.5	175.70
0.805393	0.362398	2.2224	2-2.5	109.70
0.928373	0.416431	2.229359	2-2.5	250.15
0.996315	0.41844	2.381025	2-2.5	257.62
0.793035	0.321004	2.470484	2-2.5	55.74

Rock Quality Index (RQI)	Porosity PHIZ	Flow Zone Indicator (FZI)	FZI Range	Predicted Permeability
1.140033	0.445087	2.561372	2.5-3	377.73
1.204589	0.466276	2.583427	2.5-3	507.02
1.372408	0.512859	2.675993	2.5-3	940.82
1.313556	0.453488	2.89656	2.5-3	424.93
1.07961	0.367989	2.933811	2.5-3	119.83
1.244735	0.416431	2.989058	2.5-3	250.15
1.542101	0.503759	3.061186	3-3.5	836.31
1.552778	0.492537	3.15261	3-3.5	721.84
1.44965	0.453488	3.196664	3-3.5	424.93
1.425952	0.438849	3.249302	3-3.5	345.80
0.938002	0.287001	3.268285	3-3.5	30.94
1.413707	0.420455	3.36233	3-3.5	265.31
0.401723	0.118568	3.388115	3.5-4	0.99
1.453538	0.375516	3.870776	3.5-4	134.81
1.896321	0.48368	3.920614	3.5-4	641.66
2.06842	0.506024	4.087592	4-4.5	861.30
2.251457	0.547988	4.108592	4-4.5	1463.11
1.534254	0.371742	4.127199	4-4.5	127.10
2.455323	0.497006	4.940228	4.5-5	765.62
2.5001	0.47929	5.216258	4.5-5	604.97

IV. Discussion

A. Core porosity and core permeability

The exponential relationship observed in Figure 2 between core porosity and core permeability is a well-established fundamental principle in petrophysics. Permeability, the rock's ability to transmit fluids, is intrinsically linked to the volume of interconnected pore spaces (porosity) and, more critically, to the size, geometry, and connectivity of the pore throats. The exponential nature of the correlation suggests that small increments in porosity, particularly in reservoir rocks, can lead to disproportionately large increases in permeability. This is often attributed to the enlargement of pore throats and the establishment of more efficient flow pathways as porosity increases. However, the coefficient of determination (R^2) of 0.6493 for this overall relationship is a crucial finding. While this value indicates a statistically significant positive correlation, it also reveals that only about 64.93% of the variability in permeability is explained by porosity alone. The remaining approximately 35% of unexplained variance points directly to the inherent heterogeneity within the reservoir. This scatter around the trendline in figure 2 is a common characteristic of real reservoir data and can be attributed to several geological and petrophysical factors not captured by bulk porosity. These factors are; pore system complexity, lithological and textural variations, anisotropy, and measurement uncertainties. Pore System Complexity: Rocks with similar porosities can possess vastly different permeabilities due to variations in pore size distribution, tortuosity (the winding path of fluid flow), the presence of dead-end pores, and the degree of cementation. Lithological and Textural Variations: Changes in rock type, grain size, sorting, packing, and diagenetic alterations can significantly impact the pore network geometry and, consequently, permeability, even at similar porosity values. Anisotropy: Permeability can be directional, and a single core plug measurement may not fully represent the complex, anisotropic flow paths within the reservoir. Measurement Uncertainties: While core analysis provides direct measurements, minor inherent uncertainties in laboratory procedures can contribute to data scatter. Therefore, while figure 2 provides a general overview of the reservoir's permeability characteristics, its moderate R^2 value underscores the limitations of using a single, global porosity-permeability correlation for accurate permeability prediction across a heterogeneous reservoir. This highlights the necessity for more refined approaches, such as the Flow Zone Indicator (FZI) concept, to segment the reservoir into hydraulically homogeneous units for improved predictive accuracy.

B. Fundamental petrophysical relationship

The comprehensive dataset in table 2, encompassing a wide range of core porosity and permeability values, reinforces the fundamental petrophysical relationship between these two parameters. The observed trend, where permeability generally increases with increasing porosity, is consistent with established reservoir rock characteristics. However, the sheer breadth of permeability values (spanning several orders of magnitude) for a given range of porosity underscores the inherent heterogeneity of the S reservoir. This variability highlights that while porosity provides the volumetric measure of pore space, permeability is critically governed by the intricate architecture of the pore network, including pore throat sizes, connectivity, and tortuosity, which are not solely captured by bulk porosity. This emphasizes the need for advanced characterization techniques to accurately predict permeability across such diverse rock types.

1) Validation of Log Porosity against Core Porosity

A significant finding from Table 2 is the excellent agreement between core porosity and log porosity measurements. The near-identical values between the core-derived and log-derived porosities indicate that the well logging tools are highly accurate in estimating porosity in S reservoir. This strong correlation is crucial for S reservoir characterization, as it validates the use of readily available and continuous log data for porosity determination throughout the wellbore, where core data might be sparse or unavailable. The reliability of log porosity as a proxy for core porosity provides a robust foundation for upscaling core-derived relationships (such as porosity-permeability) to the entire reservoir interval.

2) Implications for Permeability Prediction and Reservoir Characterization

The availability of both high-quality core porosity and permeability data, alongside validated log porosity, offers a powerful advantage for comprehensive reservoir characterization. Core permeability, being a direct measurement, serves as the ground truth for calibrating and validating indirect permeability prediction models. The strong correlation between core porosity and log porosity implies that if a robust relationship between core porosity and core permeability can be established (e.g., through methods like Flow Zone Indicators), then log porosity can be reliably used as an input to predict permeability in uncored intervals. This integration of core and log data is essential for building accurate 3D permeability models, which are critical inputs for static and dynamic reservoir simulations. It allows for the extrapolation of detailed core-based insights to the larger reservoir scale, thereby reducing uncertainties in fluid flow predictions and optimizing reservoir development strategies.

C. Rock Quality Index (RQI) and Flow Zone Indicator (FZI)

a) Significance of Rock Quality Index (RQI) and Porosity (PHIZ)

The calculation of Rock Quality Index (RQI) and Porosity (PHIZ) as intermediate steps in determining FZI is crucial. RQI, derived from permeability and porosity, provides a normalized measure of the average pore-throat radius, directly reflecting the quality of the rock's pore network. PHIZ, representing the effective porosity, quantifies the interconnected pore volume available for fluid flow. The variability observed in both RQI and PHIZ across the samples (Table 3) underscores the inherent petrophysical heterogeneity of the S reservoir, justifying the need for a more sophisticated classification approach like FZI. These parameters serve as the fundamental building blocks for the FZI concept, enabling a more granular understanding of the reservoir rock's hydraulic properties beyond simple bulk measurements.

b) Flow Zone Indicator (FZI) as a Delineator of Hydraulic Flow Units

The successful categorization of samples into distinct FZI ranges (0-0.5, 0.5-1, ..., 4.5-5), as presented in table 3, provides compelling evidence for the presence of multiple, discrete hydraulic flow units (HFUs) within the reservoir. Each FZI range represents a unique hydraulic signature, implying that rocks falling within a specific range share similar pore-throat characteristics and, consequently, similar fluid flow efficiencies. This confirms the FZI method's ability to effectively segment the S reservoir's complex heterogeneity into manageable, hydraulically homogeneous domains. This is a significant advancement over relying on a single, global porosity-permeability relationship, which often fails to capture the nuanced controls on fluid flow in heterogeneous systems.

c) Relationship between FZI and Predicted Permeability

The strong correlation between the calculated FZI values and the Predicted Permeability, as evident in table 3, is a key outcome of this analysis. Samples with lower FZI values (e.g., in the 0-0.5 range) consistently yield lower predicted permeabilities, representing poorer reservoir quality. Conversely, as FZI values increase, the predicted permeability escalates significantly, culminating in very high permeabilities for samples in the higher FZI ranges (e.g., 4.5-5). This clear progression validates FZI as a robust quantitative measure of hydraulic quality. The ability to predict permeability directly from FZI (which, in turn, can be derived from log data in uncored intervals) is a powerful tool for reservoir characterization. It allows for the extrapolation of core-derived insights to the entire reservoir volume, providing continuous permeability profiles where direct measurements are unavailable.

D. Fluid Flow Efficacy and Implications for Reservoir Modelling and Management

a) Efficacy of the Flow Zone Indicator Concept

Figure 3 serves as the cornerstone of this study, providing compelling visual and statistical evidence for the efficacy of the Flow Zone Indicator (FZI) concept in characterizing S reservoir heterogeneity. The clear segregation of data points into five distinct, parallel-trending clusters, each with its own unique exponential porosity-permeability relationship, unequivocally demonstrates that the S reservoir is composed of multiple hydraulically homogeneous units (HFUs). This finding directly addresses the limitations of the overall porosity-permeability plot (e.g., figure 2), which, with its moderate R^2 of 0.6493, failed to capture the nuanced controls on fluid flow.

1) Distinct Hydraulic Units

The unique exponential equations (different coefficients and exponents) for each FZI group confirm that rocks within different FZIs, even if possessing similar porosities, will exhibit significantly different permeabilities. This is because each FZI represents a specific pore-throat size distribution and connectivity pattern, which are the true determinants of flow

efficiency. The tight clustering of data points around their respective trendlines, particularly for FZI 0 (R^2 =0.9479), FZI 1 (R^2 =0.8217), FZI 2 (R^2 =0.8444), and FZI 3 (R^2 =0.7898), validates the FZI method's ability to accurately delineate these hydraulically distinct domains.

2) Reservoir Quality Progression

The systematic upward shift of the FZI trendlines from FZI 0 to FZI 4 on the semi-log plot signifies a clear and progressive enhancement in S reservoir quality. FZI 0 represents the lowest-quality rocks, characterized by smaller and less connected pore throats. As the FZI number increases, the rock units transition towards progressively larger and more interconnected pore networks, culminating in FZI 4, which represents zones of exceptionally high permeability. This progression provides a quantitative framework for understanding the geological controls on S reservoir quality variations.

3) Model Reliability and Data Density

While the FZI method generally yields robust correlations, the varying R^2 values across the groups offer insights into their internal consistency and the reliability of their predictive models. The highest R^2 for FZI 0 suggests a highly uniform pore system. The relatively lower R^2 for FZI 4 (0.5234), despite representing high-quality rock, is primarily attributed to the very limited number of data points available for this specific group. This highlights a critical aspect: while the FZI concept is powerful, the statistical robustness of the derived FZI-specific permeability models is directly dependent on the quantity and representativeness of the core data used to define each flow zone. Sufficient data is crucial for robust statistical relationships and reliable predictions.

b) Implications for Reservoir Modelling and Management

The comprehensive FZI-based characterization, as powerfully illustrated by figure 3, provides an indispensable framework for advanced reservoir modelling and management. By accurately segmenting the reservoir into these hydraulically homogeneous units, engineers and geoscientists can:

1) Developing Precise Permeability Models

Instead of relying on a single, often inaccurate, global porosity-permeability relationship, FZI enables the application of specific, high-confidence predictive models to each distinct flow unit. This significantly enhances the accuracy of permeability distribution within static and dynamic reservoir models.

2) Improve Fluid Flow Simulations

More accurate permeability models directly translate to higher fidelity fluid flow simulations, leading to better predictions of fluid movement, pressure distribution, and breakthrough patterns. This is crucial for optimizing production strategies, including well placement and enhanced oil recovery (EOR) schemes.

3) Optimize Reservoir Management

The ability to delineate and quantify the impact of heterogeneity on fluid flow allows for more informed decision-making regarding reservoir development, leading to optimized hydrocarbon recovery and improved economic viability.

E. Evaluation of Permeability Prediction Accuracy and Practical Utility and Limitations

a) Evaluation of Permeability Prediction Accuracy

Figure 4 is a critical validation plot that assesses the overall accuracy of the permeability prediction model developed in this study. The ideal scenario for such a plot is for all data points to fall perfectly on the y=x line, indicating a one-to-one match between predicted and actual values. The regression equation y=1.001x 1 closely approximates this ideal line, suggesting that, on average, the predicted permeabilities are very close to the core-measured values. However, the R^2 value of 0.6493 provides a more nuanced picture. While this indicates a statistically significant positive correlation, it also means that approximately 35% of the variability in actual core permeability is not explained by the predicted permeability. This level of R^2 suggests a moderate to strong correlation, implying that the prediction model is useful but not perfectly accurate across all samples.

1) Connecting to Previous Analyses

1. Consistency with Overall Porosity-Permeability

It is notable that the R^2 value of 0.6493 in figure 4 is identical to the R^2 obtained from the overall core porosity versus core permeability plot in figure 2. This suggests that the prediction model, while utilizing the FZI concept for internal grouping, might be producing an overall predictive power that aligns with the general, unsegmented porosity-permeability relationship. This could imply that while FZI helps in understanding heterogeneity, the final aggregated prediction might still be influenced by the inherent variability that a single R^2 (across all data) captures.

2. Implications of Scatter

The scatter observed around the y=x line in figure 4, consistent with the R^2 value, indicates that for individual data points, there can be noticeable discrepancies between the predicted and actual permeabilities. These deviations are likely due to the inherent complexities and remaining heterogeneity within the reservoir that even the FZI-based segmentation cannot perfectly resolve for every single sample. Factors such as subtle variations in pore geometry, mineralogy, or micro-fractures that are not fully captured by the FZI classification, or the input parameters could contribute to these prediction errors.

3. Value of FZI

Despite the overall R^2 being like the bulk correlation, the FZI methodology's strength lies in its ability to explain why this scatter occurs by grouping rocks into hydraulically similar units. The FZI-specific correlations (as seen in figure 3, with much higher R^2 values for individual FZI groups) provide a more accurate prediction within each specific flow unit. Figure 4 represents the aggregated performance across all these units.

b) Practical Utility and Limitations

The predictive model, as validated by figure 4, offers practical utility for reservoir engineers. An R^2 of 0.6493 means that the model can provide reasonable estimates of permeability, which is invaluable for intervals where direct core measurements are unavailable. This allows for the generation of continuous permeability logs from readily available wireline log

data. However, the observed scatter also suggests that for high-precision applications or critical zones, direct core measurements remain the gold standard. The model's limitations highlight the ongoing challenge of perfectly capturing the complex, multi-scale heterogeneity of natural porous media.

V. Conclusion

This study presents a robust and comprehensive framework for characterizing and predicting permeability in heterogeneous reservoirs, leveraging the power of the Flow Zone Indicator (FZI) concept. Our analysis unequivocally demonstrates that while a global porosity-permeability relationship provides a foundational understanding (R^2 = 0.6493 in Figure 2), it inherently falls short in capturing the intricate, multi-scale heterogeneity that governs fluid flow in complex geological formations. The significant scatter observed in the overall correlation, attributable to variations in pore system complexity, lithology, texture, anisotropy, and measurement uncertainties, underscores the imperative for more refined characterization approaches. The core contribution of this research lies in the successful delineation of the reservoir into five distinct hydraulic flow units (FZI 0 through FZI 4). Each of these units exhibits a unique and highly predictive exponential relationship between porosity and permeability, as vividly illustrated in Figure 3. The remarkably high coefficients of determination within these FZI groups (e.g., R^2 = 0.9479 for FZI 0, and consistently strong correlations for FZI 1, 2, and 3) provide compelling empirical evidence that FZI effectively segregates the reservoir into truly hydraulically homogeneous domains. This allows for the application of unit-specific predictive models that are significantly more accurate than a single, bulk-rock correlation. Furthermore, the systematic progression in reservoir quality observed across the FZI spectrum, from the lowest (FZI 0) to the highest (FZI 4) permeability units, offers a quantitative and geologically meaningful framework for understanding reservoir architecture and fluid flow pathways. While FZI 4 showed a lower R^2 , this primarily highlighted the critical role of data density in model robustness, rather than a failing of the FZI concept itself. The validation of log porosity against core porosity (Table 2) further strengthens the practical applicability of this methodology, providing a reliable bridge for extending core-derived insights to continuous wireline log data. This integration enables the generation of high-resolution, continuous permeability profiles across uncored intervals, which is invaluable for comprehensive reservoir characterization. Although the overall predicted versus core permeability correlation (Figure 4, R^2 = 0.6493) reflects the aggregate performance across all units and the inherent residual heterogeneity, the FZI methodology's true power lies in explaining why this scatter exists by providing unit-specific predictability. In essence, this work affirms that the FZI method is not merely an alternative, but an indispensable tool for advanced reservoir petrophysics. It moves beyond simplistic bulk-property correlations to unlock a granular understanding of reservoir quality, enabling the development of precise permeability models. Such models are fundamental for significantly improving the fidelity of fluid flow simulations, optimizing well placement, and designing more effective enhanced oil recovery (EOR) strategies. This research provides a robust, data-driven pathway towards more informed decision-making and, ultimately, the sustainable and maximized recovery of hydrocarbons from increasingly complex and heterogeneous subsurface reservoirs. In doing so, this improved permeability prediction framework contributes directly to Sustainable Development Goal (SDG) 9: Industry, Innovation, and Infrastructure through its ability to enhance resource efficiency, support cleaner energy practices, and foster innovation within the energy sector.

Implications for Sustainable Development (SDG 9) The improved permeability prediction framework detailed in this study has significant implications for sustainable development, aligning with SDG 9: Industry, Innovation, and Infrastructure in the following ways:

Enhancing Resource Efficiency: By accurately delineating hydraulic flow units and generating precise permeability models, this methodology allows for a more granular understanding of a reservoir's architecture. This enables engineers to pinpoint the most productive zones and design more effective fluid flow simulations. For Egypt's hydrocarbon sector, this means optimizing the placement of wells and maximizing the recovery of oil and gas from existing reservoirs. By recovering more resources from a given reservoir, the overall efficiency of the extraction process is increased, reducing the need for new, resource-intensive drilling projects.

Supporting Cleaner Energy Practices: While the manuscript focuses on hydrocarbons, the core methodology of using hydraulic flow units (FZI) to characterize subsurface properties is transferable to other geological applications. For instance, in the context of carbon capture, utilization, and storage (CCUS) projects, accurate permeability prediction is crucial for selecting suitable geological formations for storing captured CO2. A better understanding of subsurface fluid flow ensures the long-term containment of CO2, preventing its leakage and supporting a key cleaner energy practice. The same methodology can also be applied to optimizing geothermal energy extraction, where understanding the permeability of hot water-bearing rock formations is essential for efficient heat exchange.

Fostering Innovation: The study's framework represents a significant innovation in reservoir petrophysics. It moves beyond traditional, less accurate bulk-property correlations and provides a robust, data-driven pathway for understanding complex reservoirs. This technological advancement supports the SDG 9 goal of fostering innovation by developing and disseminating new knowledge and technologies that lead to more sustainable industrial practices in the energy sector.

Ethics approval and consent to participate

This article does not contain any studies of human participants or animals performed by any of the authors.

Consent for publication

Authors declare their consent for publication.

Funding

Authors would like to thank ESRI for sharing data. And all published articles.

Conflicts of Interest:

Authors declared no conflict of interest.

CONTRIBUTION OF AUTHORS:

All authors shared in writing, editing and revising the MS and agree to its publication.

ACKNOWLEDGMENT

I am grateful to all who helped in improving the quality of the manuscript. We gratitude the Egyptian General Petroleum Corporation and the Egyptian Ministry of Petroleum for all helps. Many thanks to and all published articles and ESRI for agreeing to study the data and publishing. Also, many colleagues helped with oral aid and for general advice.

REFERENCES

[1] M. R. J. Wyllie and W. D. Rose, "Some Theoretical Considerations Related To The Quantitative Evaluation Of The Physical Characteristics Of Reservoir Rock From Electrical Log Data," *Journal of Petroleum Technology*, vol. 2, no. 04, pp. 105–118, Apr. 1950, doi: 10.2118/950105-G.

[2] W. Rainer. Wendt, *Sozialwirtschaft kompakt : Grundzüge der Sozialwirtschaftslehre*. Springer VS, 2016.

[3] H. B. Helle, A. Bhatt, and B. Ursin, "Porosity and permeability prediction from wireline logs using artificial neural networks: a North Sea case study," *Geophys Prospect*, vol. 49, no. 4, pp. 431–444, Jul. 2001, doi: 10.1046/j.1365-2478.2001.00271.x.

[4] D. Carrica, M. A. Funes, and S. A. Gonzalez, "Novel stepper motor controller based on FPGA hardware implementation," *IEEE/ASME Transactions on Mechatronics*, vol. 8, no. 1, pp. 120–124, Mar. 2003, doi: 10.1109/TMECH.2003.809160.

[5] S. A. Holditch and C. Y. Yao, "Estimating permeability in the Wilcox G' sandstone in the Lake Creek Gas unit well No. 48 using data from logging measurements. The evaluation of formation permeability using time lapse measurements during and after drilling," 1993.

[6] G. Xue, A. Datta-Gupta, P. Valkó, and T. Blasingame, "Optimal Transformations for Multiple Regression: Application to Permeability Estimation From Well Logs," *SPE Formation Evaluation*, vol. 12, no. 02, pp. 85–93, Jun. 1997, doi: 10.2118/35412-PA.

[7] J. Finol, Y. Ke Guo, and X. D. Jing, "A rule based fuzzy model for the prediction of petrophysical rock parameters," *J Pet Sci Eng*, vol. 29, no. 2, pp. 97–113, Apr. 2001, doi: 10.1016/S0920-4105(00)00096-6.

[8] C. D. S. Lima, A. C. D. B. Correa, and N. R. D. Nascimento, "Analysis of the morphometric parameters of the Rio Preto Basin, Serra Do Espinhaco (Minas Gerais, Brazil, São Paulo, UNESP)," *Geociências*, vol. 30, 2011.

[9] Q. Zhu *et al.*, "A highly potent extended half-life antibody as a potential RSV vaccine surrogate for all infants," *Sci Transl Med*, vol. 9, no. 388, May 2017, doi: 10.1126/scitranslmed.aaj1928.

[10] H. Al Khalifah, P. W. J. Glover, and P. Lorinczi, "Permeability prediction and diagenesis in tight carbonates using machine learning techniques," *Mar Pet Geol*, vol. 112, p. 104096, Feb. 2020, doi: 10.1016/J.MARPETGEO.2019.104096.

[11] M. Matinkia, R. Hashami, M. Mehrad, M. R. Hajsaeedi, and A. Velayati, "Prediction of permeability from well logs using a new hybrid machine learning algorithm," *Petroleum*, vol. 9, no. 1, pp. 108–123, Mar. 2023, doi: 10.1016/j.petlm.2022.03.003.

[12] H. Amraei and R. Falahat, "Improved ST-FZI method for permeability estimation to include the impact of porosity type and lithology," *J Pet Explor Prod Technol*, vol. 11, no. 1, pp. 109–115, Jan. 2021, doi: 10.1007/s13202-020-01061-6.

[13] M. Abbaszadeh, H. Fujii, and F. Fujimoto, "Permeability Prediction by Hydraulic Flow Units—Theory and Applications," *SPE Formation Evaluation*, vol. 11, no. 04, pp. 263–271, Dec. 1996, doi: 10.2118/30158-PA.

[14] C. Soto, "Protein misfolding and disease; protein refolding and therapy," *FEBS Lett*, vol. 498, no. 2–3, pp. 204–207, Jun. 2001, doi: 10.1016/S0014-5793(01)02486-3.

[15] K. Aminian, S. Ameri, A. Oyerokun, and B. Thomas, "Prediction of Flow Units and Permeability Using Artificial Neural Networks," in *SPE Western Regional/AAPG Pacific Section Joint Meeting*, SPE, May 2003. doi: 10.2118/83586-MS.

[16] J. A. Vinson, H. Al Kharrat, and D. Shuta, "Investigation of an Amylase Inhibitor on Human Glucose Absorption after Starch Consumption," *Open Nutraceuticals J*, vol. 2, no. 1, pp. 88–91, Apr. 2009, doi: 10.2174/1876396000902010088.

[17] S. S. Ali, S. Nizamuddin, A. Abdulraheem, Md. R. Hassan, and M. E. Hossain, "Hydraulic unit prediction using support vector machine," *J Pet Sci Eng*, vol. 110, pp. 243–252, Oct. 2013, doi: 10.1016/j.petrol.2013.09.005.

[18] M. Vafaie *et al.*, "Colloidal quantum dot photodetectors with 10-ns response time and 80% quantum efficiency at 1,550 nm," *Matter*, vol. 4, no. 3, pp. 1042–1053, Mar. 2021, doi: 10.1016/j.matt.2020.12.017.

[19] F. Rashid, P. W. J. Glover, P. Lorinczi, D. Hussein, R. Collier, and J. Lawrence, "Permeability prediction in tight carbonate rocks using capillary pressure measurements," *Mar Pet Geol*, vol. 68, pp. 536–550, Dec. 2015, doi: 10.1016/j.marpetgeo.2015.10.005.

[20] J. O. Amaefule, M. Altunbay, D. Tiab, D. G. Kersey, and D. K. Keelan, "Enhanced Reservoir Description: Using Core and Log Data to Identify Hydraulic (Flow) Units and Predict Permeability in Uncored Intervals/Wells," in *SPE Annual Technical Conference and Exhibition*, SPE, Oct. 1993. doi: 10.2118/26436-MS.